Study of Mild Traumatic Brain Injuries Using Experiments and Finite Element Modeling

Michael Lamy, Daniel Baumgartner and Remy Willinger
University of Strasbourg, France

Narayan Yoganandan and Brian D. Stemper
Medical College of Wisconsin, Milwaukee, USA

ABSTRACT – The objective of the study was to better understand the biomechanics of mild traumatic brain injuries (TBI) using a hybrid approach: experiments and computational modeling. A three-dimensional finite element model of the rat skull and brain was used to understand the anatomical region-dependent stress response under mild TBI conditions. Anesthetized rats were exposed to varying coronal plane angular acceleration pulses without direct head contact. Experimental outcomes included unconscious time and histological evidence of brain pathology using GFAP and MAP2. The finite element model was exercised using the five experimental and four supplemental pulses to simulate nine independent combinations of peak acceleration and pulse duration (290 to 542 krad/s² and 1 to 3 ms). Stress response metrics were correlated to histological and behavioral (e.g., loss of consciousness) evidence of injury in rats subjected to pure coronal plane angular acceleration of the head. Injury severity was modulated by independently controlling peak magnitude and duration of the angular acceleration. While peak Von Mises stresses correlated well with changes in injury severity associated with peak angular acceleration, this metric did not demonstrate sensitivity to changes in acceleration duration. However, an integrated stress-time metric was able to predict changes in injury severity associated with increasing angular acceleration magnitude and duration in both the hippocampal and parietal cortex anatomical regions. Results of this unique hybrid analysis indicate that the combined stress-time variable may be more suited to explain variation of mild TBI severity, rather than pure peak metrics.

INTRODUCTION

Traumatic brain injuries (TBI) are a major cause of disability/death in Western societies. A recent review indicated that the annual incidence of hospitalization for TBI was 235 and 103 per 100,000 in Europe and the United States, respectively (Tagliaferri et al., 2006). In terms of demographics, young adults appear to be the primary victims, a phenomenon which results in considerable costs for society. The main causes for TBI are motor vehicle collisions, falls, and sports-related activities. Modern protective systems and structures in automotive environments have decreased the mortality rate for TBI cases. Such systems generally aim at reducing the risks of moderate to severe injuries. However, more than 70% of the TBI are classified as mild (Cassidy et al., 2004). Though less likely to lead to death, mild TBI can be responsible for lifelong disabilities, resulting in significant public health issues.

Impacts and complex loading conditions have long been postulated as mechanisms of TBI. In particular, the accelerations sustained by the head in these solicitations have been studied in depth. In real life collisions, the loading consists of linear and rotational accelerations. Although head injuries are obviously a consequence of both components, they are generally studied separately to determine their respective influences. Linear accelerations have been shown to produce focal brain injuries, correlated to intracranial pressure changes (Lissner et al., 1960). Linear acceleration is a main feature of the Head Injury Criterion (NHTSA, 2003). However, angular accelerations are also important in brain injury mechanisms (Holbourn, 1943). Some studies have reported that angular acceleration has a greater contribution to injury occurrence than linear acceleration (Gennarelli et al., 1981; Gennarelli et al., 1982; Zhang et al., 2006). A majority of previous studies have focused on AIS 4-6 trauma (Gennarelli and Wodzin, 2006).

These observations demonstrate the need for studies on the role of angular acceleration in producing mild TBI (AIS 2-3) and modulating severity. Animal models demonstrating physiological and behavioral deficits are crucial because mild TBI outcomes are more subtle than moderate or severe cases. The rat model is widely used in Neurotrauma research as loading conditions can be precisely controlled.

CORRESPONDING AUTHOR:
Michael Lamy, PhD, Institute for Fluid and Solid Mechanics, University of Strasbourg, 2 Rue Boussingault, Strasbourg, France; Email: michael.lamy@unistra.fr

Graded behavioral and pathological responses have been outlined. Such experiments can be used to drive computational simulations such as Finite Element Models (FEM). These models are used to better determine tissue-level behaviors of various brain structures (hippocampus, parietal cortex, etc). Thus, an approach combining an animal model of closed head injury in the rat and a FEM of the rat brain was used to better understand the biomechanical response of the brain specific to mild TBI.

METHODS

Mild TBI was induced in rats through coronal plane head angular acceleration (Fijalkowski et al., 2007). The experimental model consisted of a helmet that fit securely on the rat head with a laterally extended moment arm. The anterior helmet portion was attached to the test frame using a pin joint that permitted only coronal plane rotation about an axis centered on the cervical spine. An impactor was accelerated in a guide tube to impact the helmet moment arm resulting in helmet rotation. Impact characteristics, and therefore, helmet angular acceleration characteristics, were controlled by initial drop height of the impactor and an elastomer placed on the impacting surface of the helmet moment arm (Fijalkowski et al., 2006). Helmet kinematics were recorded using high-speed videography and filtered using a cohert analysis technique (Fijalkowski et al., 2009a).

The protocol for adult male Sprague Dawley rats consisted of administration of general anesthesia using ketamine (75 mg/kg) and medetomidine (0.5 mg/kg). This protocol was shown to have a limited effect on neurological function (Hahn et al., 2005; Sun et al., 2003). Rats became unresponsive after approximately ten minutes. They were then placed in the helmet and exposed to angular accelerations. Immediately following the insult, rats were given a reversal agent to counteract effects of anesthesia. Unconscious time was assessed as the time from reversal agent administration to return of the corneal reflex.

Each rat was exposed to a single head angular acceleration event. The pulse was characterized according to peak angular acceleration and positive duration (Figure 1). Positive duration was defined as the duration between zero crossings of the positive angular acceleration pulse. Peak angular acceleration and positive duration were independently varied to determine effects of each of these characteristics on injury severity. Peak angular acceleration was varied to three levels (M1, M2, M3) while maintaining positive duration at the same level (D2). Likewise, positive duration was varied to three levels (D1, D2, D3) while maintaining peak angular acceleration at the same level (M2). This matrix resulted in a total of five different experimental groups: M1D2, M2D2, M3D2, M2D1, and M2D3. Six rats were included in four of the experimental groups, whereas seven rats were included in the M2D2 group.

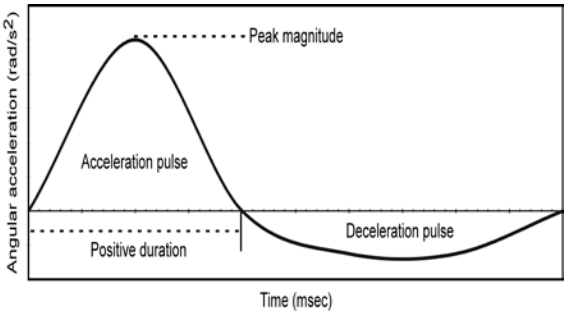

Figure 1: Head angular acceleration versus time pulse theoretical characteristics.

Control and experimental rats were sacrificed 24 hours after injury or sham procedure with an overdose of sodium pentobarbital (100mg/kg IP). The extracted brain was fixed using 4% paraform-aldehyde, cryoprotected in 30% sucrose for 24 hours, and stored at -80 deg C. Coronal cryostat sections (10 μm) were obtained between the olfactory bulbs and paramedian lobule. Autofluorescence techniques were incorporated to evaluate subtle evidence of brain trauma. Mid-brain coronal sections were used to analyze the distribution of MAP2 and GFAP immunoreactivity. Immunohistochemistry focused on the hippocampus and parietal cortex regions.

Finite Element Model

A Finite Element Model (FEM) of the rat brain was developed to simulate the five experimental pulses. It was based upon animal geometry which was acquired from medical imaging techniques. Rat skull geometry was obtained from micro-Computed Tomography images (voxel size: 93 μm x 93 μm x 93 μm), and the soft tissue geometry was extracted from Magnetic Resonance Images (voxel size 500 μm x 500 μm x 500 μm). Thresholding techniques were used to define external surfaces of the brain.

This surface served to delimit the volume that had to be meshed to represent the brain in the FEM. The meshing task was performed with the ALTAIR HYPERMESH 10.0 © software. The final mesh consisted of six anatomical regions: cerebrum, cerebellum, brainstem, olfactory bulbs, rigid skull,

and a layer of elements between the brain and the skull. The cerebrum was subdivided into 18 anatomical components to permit better spatial definition of soft tissue stresses within the brain. The components consisted of the orbitofrontal, cingulate, parietal, temporal, occipital and entorhinal cortexes; striatum, septum, thalamus, amygdale, hypothalamus, hippocampus, mesencephalic tegmentum, ventral tegmental nuclei, superior and inferior colliculous, aqueduct, and subiculum. The composite FE mesh was continuous and composed of 17,972 hexahedral HEPH (Radioss, 2009) elements (all components except the skull) and 3,220 shell elements (skull). The average edge size was 0.45 mm, and warpage and skewness indexes were taken into account during creation to ensure that the shape of the hexahedral elements were acceptable.

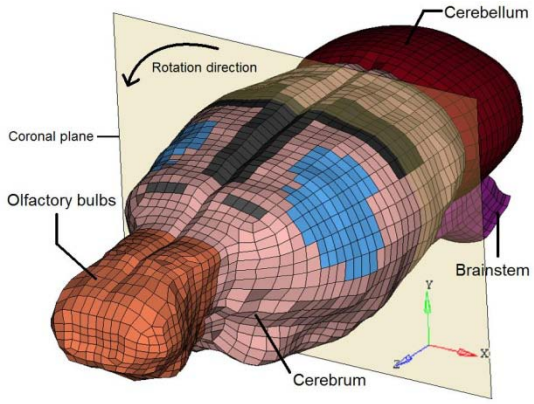

Figure 2: The Rat Brain FEM

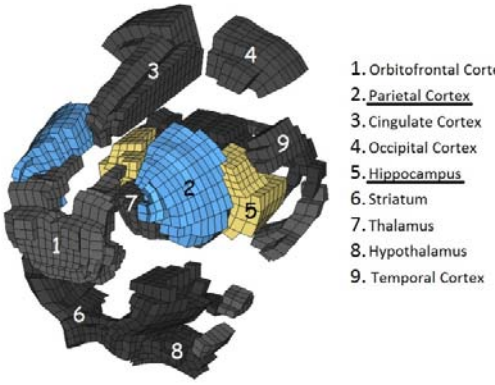

Figure 3: Exploded view of the cerebrum subdivisions (only the main visible components are listed in the legend)

The second step in the creation of the FEM consisted of tissue property definition. This was performed using ALTAIR HYPERCRASH 10.0 © software. All the elements of the model were considered to be homogeneous and isotropic. Moreover, all brain elements were depicted as gray matter. Soft tissue mechanical behaviors were obtained from data reported in literature. The skull and the brain/skull interface were attributed a linear elastic behavior, with properties respectively based upon studies from (Baumgartner and Willinger, 2004) and (Mao et al., 2006).

Table 1: Material properties of the skull and brain/skull interface.

	Young modulus (MPa)	Poisson's ratio	Density (kg/m^3)
Skull	15,000	0.21	1,800
Brain/skull interface	20	0.45	1,130

The other components of the model, i.e. those representing the brain itself, were assigned a linear viscous elastic material behavior. The Boltzman law was chosen to represent this behavior, and the associated mechanical parameters were based upon the suggestions of (Fijalkowski et al., 2009b).

Table 2: Properties of the brain material.

Short term shear modulus	Long term shear modulus	Bulk modulus	Decay constant	Density
kPa	kPa	GPa	S^{-1}	$kg.m^{-3}$
10	2	2.19	0.125	1,040

Numerical Simulation

The five experimental groups were simulated with the FEM. Coronal plane angular acceleration versus time pulse was defined as the applied load case for each group based upon experimentally measured acceleration data (Figure 4). Tissue-level stress response was compared to experimentally-derived pathological outcomes as well as injury severity graded as unconscious times. The FEM was subjected to four additional angular acceleration pulses, independent of the simulation of experimental outcomes from five angular acceleration pulses. The four supplemental pulses were termed as M1D1, M1D3, M3D1 and M3D3, for a total of nine pulses. These nine pulses constituted all combinations of three acceleration magnitudes and three durations (Table 3). It should be noted that histological, anatomical, and behavioral studies were not available for these four supplemental pulses.

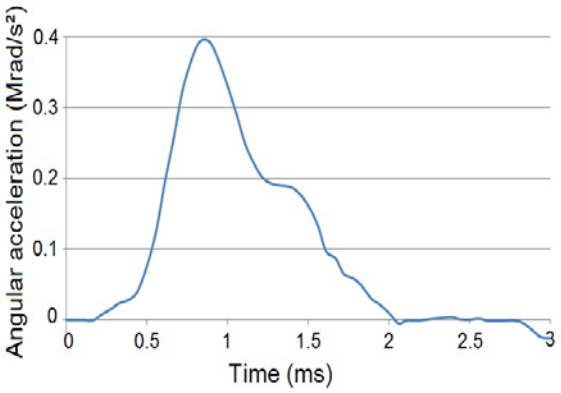

Figure 4: Representative angular acceleration versus time input (M2D1 case).

Table 3: Complete set of acceleration pulses amplitudes and durations. In each cell, numbers on top indicate angular acceleration (krad/s²) and numbers on the bottom indicate duration (ms).

	M1	M2	M3
D1	292 1.0	424 1.1	543 1.2
D2	292 2.1	419 2.0	523 2.0
D3	292 3.0	427 3.0	533 3.0

Apart from the loading conditions, the properties of the model were unchanged between the experimental and supplemental simulations. Computations were performed using the RADIOSS CRASH © solver. Among the computed outcomes, Von Mises stresses were given particular interest, having been identified as possible relevant parameters (Baumgartner et al., 2009). It should be noted that many studies have indeed proposed Von Mises stresses as an injury criterion (Baumgartner and Willinger, 2004; Marjoux et al., 2008). For every parameter, time history data as well as anatomical distribution in the brain model were analyzed to determine the outcomes of the acceleration-induced mechanical response. The biomechanical parameters of interest such as Von Mises stress were output for each element. The mean stress value of all elements for each anatomical region was determined as a function of time. The peak value was extracted from the mean value versus time history curve.

RESULTS

Thirty-one rats were exposed to the experimental protocol and sustained mTBI without skull fracture or cervical spine injury. Following brain injury and administration of reversal agent, all rats fully recovered according to the following criteria: return of the corneal reflex and ability to ambulate. All control rats survived the sham procedure and fully recovered. Each experimental group was subjected to head angular acceleration pulses with differing peak and duration (Table 4). Return of corneal reflex was used to assess unconscious time. Unconscious times increased in experimental rats for groups exposed to greater peak angular acceleration magnitude and greater positive duration (Table 4).

Table 4: Mean ± standard deviations for experimental pulse characteristics (α: angular acceleration, UT: unconscious time).

	M1D2	M2D2	M3D2	M2D1	M2D3
α (krad/s²)	292±34	419±29	523±15	424±24	427±21
Duration (ms)	2.1±0.2	2.0±0.2	2.0±0.2	1.1±0.2	3.0±0.1
UT (s)	206±44	366±25	445±28	200±12	630±105

Numerical Results

The lower part of the hippocampus was observed to be the region where maximal Von Mises stresses were located. Other potential maximal values were identified in the lower cerebrum but appeared in locations with strong curvatures imposed by the rigid skull; moreover, these values generally concerned isolated elements, therefore they were not deemed to be as important as hippocampal stresses. The parietal cortex also displayed the presence of large Von Mises stresses, but of slightly lesser magnitude than in the hippocampus.

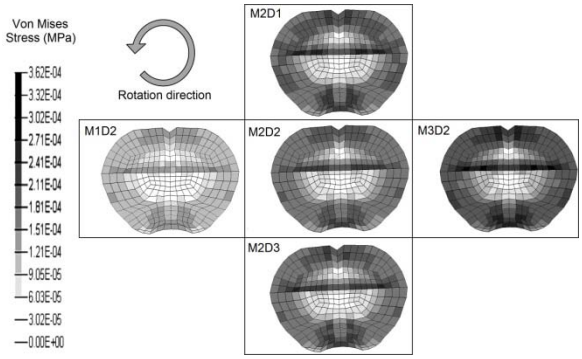

Figure 5: Coronal section of the model demonstrating Von Mises stresses for each experimental pulse.

Figure 5 displays the same coronal plane section for all five experimental pulses. Each image corresponds

to the instant when maximal Von Mises stress was observed in the hippocampus. It must be noted that maximum stress values occurred approximately simultaneous (less than 0.1 ms delay) with the peak angular acceleration.

Relationship of Pathological Findings to Stress Outputs in the Hippocampal Region

Figure 6 demonstrates the relationship between peak Von Mises stress, stress-time, and experimental outcomes for all five experimental groups. GFAP reactivity, indicating reactive astrocytosis, was evident primarily in the hippocampal anatomical region. Evidence of astrocytosis was greater in brain sections from rats exposed to longer duration (e.g., M2D3) and higher peak angular accelerations (e.g., M3D2), shown in Figure 6. Brain sections from rats exposed to low peak magnitude or short duration angular accelerations had minimal evidence of reactive astrocytosis and microscopic images were not remarkably different from controls. A clear trend of increasing injury severity was apparent with increasing positive duration (M2D1 to M2D2 to M2D3). The trend was not as apparent for increasing peak magnitude.

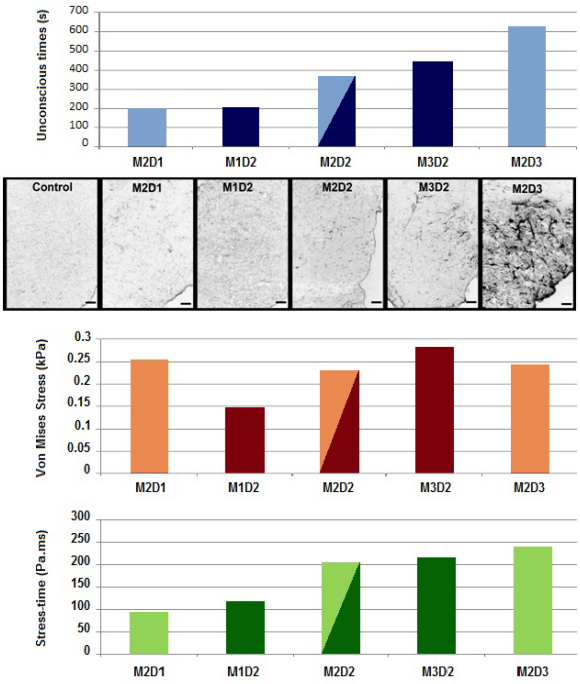

Figure 6: Comparison of results from the five experimental groups in the hippocampus region. Shown from top to bottom are the loss of consciousness times, GFAP immunohistochemistry, peak Von Mises stresses, and stress-time responses.

For the present comparison, peak Von Mises stresses were quantified in the hippocampus region. Peak Von Mises stresses increased with greater angular acceleration magnitudes (M1D2 to M2D2 to M3D2). However, a similar trend was not observed for increasing acceleration duration (M2D1 to M2D2 to M2D3).

As a consequence, a new metric was evaluated to account for the combined influence of amplitude and duration. This was accomplished through the use of a stress-time parameter. The mean Von Mises stress data history was integrated in the anatomical region of interest. Then the stress-time value was defined as the integral for the duration of the pulse. The asset of this metric was to inherently add a shape factor to the basic peak stress, by implicitly incorporating duration. Figure 6 demonstrates consistency between unconscious times, GFAP evidence of reactive astrocytosis, and the Von Mises stress-time metric with regard to changes in magnitude and duration of the applied angular acceleration pulse.

Relationship of Pathological Findings to Stress Outputs in the Parietal Cortex Region

Figure 7 demonstrates the relationship between peak Von Mises stress, stress-time, and experimental outcomes for all five experimental groups. Structural damage was identified using MAP2 staining. MAP2 reactivity was evident primarily in the parietal cortex. As with GFAP staining, greatest evidence of injury was identified in rats subjected to accelerations with higher peak magnitudes (e.g., M3D2) or longer durations (e.g., M2D3). Greater evidence of injury was apparent for lower magnitude and shorter duration pulses than with GFAP staining. However, graded evidence of increasing injury severity was apparent in the parietal cortex for increasing magnitude (M1D2 to M2D2 to M3D2) and duration (M2D1 to M2D2 to M2D3).

For the present comparison, Von Mises stress magnitude and stress-time metrics were quantified in the parietal cortex anatomical region. While a clear trend was evident for peak Von Mises stress with increasing angular acceleration magnitude, stress magnitude did not increase with increasing pulse duration. However, Von Mises stress-time metric increased with increasing magnitude and duration of the angular acceleration pulse. This finding agreed with GFAP (hippocampus) and MAP2 (parietal cortex) histological evidence of injury. As with GFAP staining, the Von Mises stress-time metric correlated with MAP2 histological evidence of injury better than the peak Von Mises stress (Figure 7).

The stress-time metric showed better correlation with experimental unconscious times than peak Von Mises stress. Table 5 shows results of a linear correlation analysis demonstrating that unconscious times increase in a predictable manner with the reported stress-time values.

Peak Stress Analysis Using Supplementary Pulses

The model was exercised beyond the range of experimental pulses using four supplementary angular acceleration pulses to complete the 3x3 test matrix. Peak Von Mises stress and stress-time metrics were compared across the nine groups of acceleration pulses. The left column of figure 8 sorts the nine groups by similar acceleration amplitudes (approximately 290 krad/s² for M1 cases, 420 krad/s² for M2 cases, and 530 krad/s² for M3 cases). Thus, groups can be compared by the duration of the acceleration pulse. Von Mises stresses were greatest in the hippocampus anatomical region and tended to decrease with increasing pulse duration. This finding is inconsistent with trends observed in Figures 6 and 7.

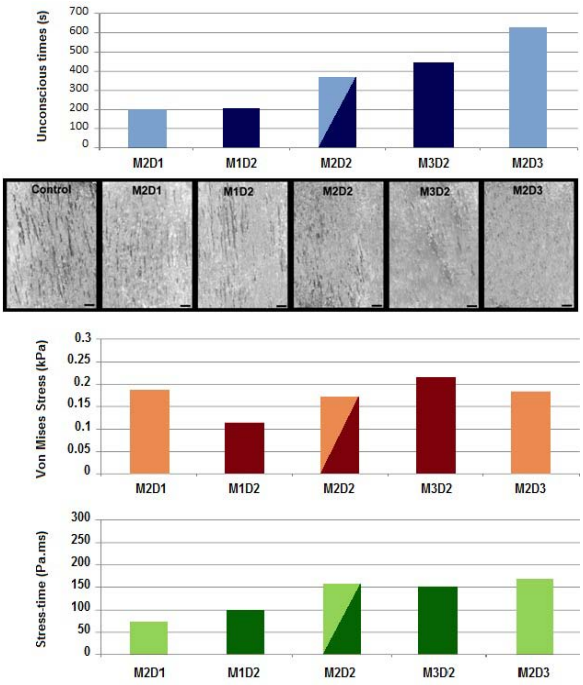

Figure 7: Comparison of results from the five experimental groups in the parietal cortex region. Shown from top to bottom are the loss of consciousness times, MAP2 immunohistochemistry, peak Von Mises stresses, and stress-time responses.

Table 5: Correlations of stress response to unconscious times.

Variable	Region	Slope	R^2
Stress-time	Hippocampus	2.612	0.8651
	Parietal cortex	3.793	0.7795
Von Mises stress	Hippocampus	1.672	0.217
	Parietal cortex	2.423	0.2452

The right column of figure 8 sorts the nine experimental groups by similar acceleration durations (1 ms for D1 cases, 2 ms for D2 cases, and 3 ms for D3 cases). Stresses can be compared by the amplitude of the initially applied acceleration pulse. Peak stresses occurred in the hippocampus region. The most relevant information gathered from these results is that the Von Mises stresses in the brain increase with the amplitude of the solicitation, for a given duration. This is observed for each of the three duration groups and is consistent with trends observed in Figures 6 and 7.

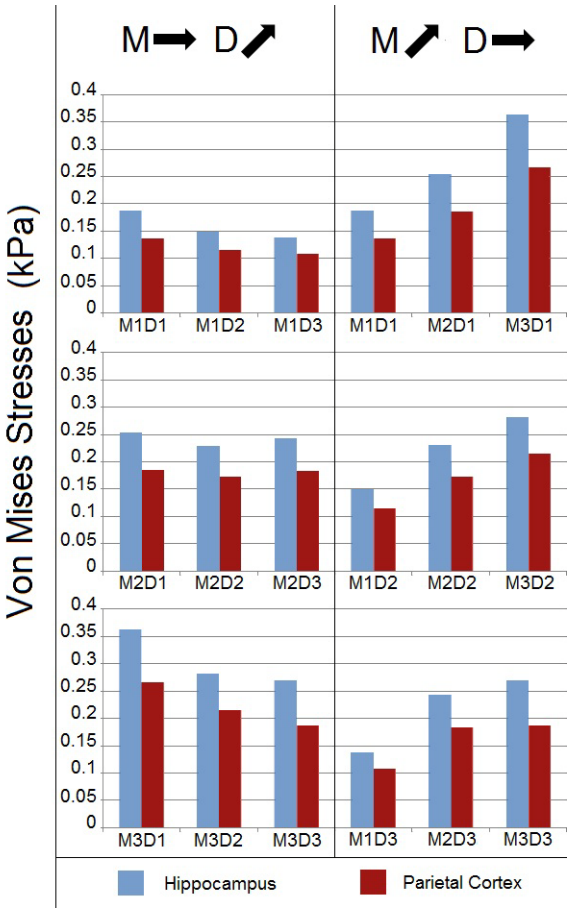

Figure 8: Numerical Von Mises stresses for the nine angular acceleration pulses.

Stress-Time Analysis Using Supplementary Pulses

Similarly to Figure 8, the left column of Figure 9 sorts the nine experimental groups by similar amplitudes and increasing pulse durations, while the right column does the opposite (fixed durations, increasing amplitudes). The stress-time metric responded similarly to the peak Von Mises stress metric with increasing acceleration magnitude. With regard to duration, the influence on stress-time was opposite, i.e., while stresses decreased, the stress-time response increased with duration. These findings are more consistent with trends observed in Figures 6 and 7.

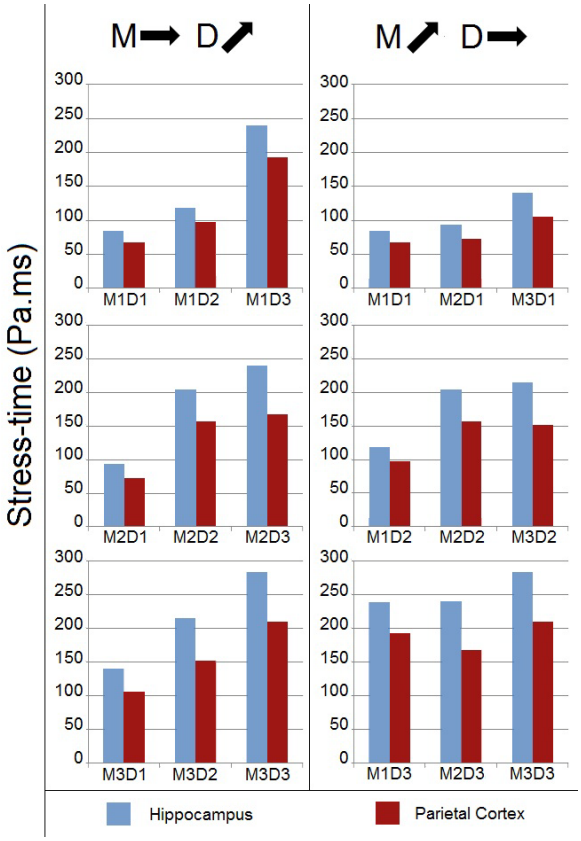

Figure 9: Numerical stress-time for the nine angular acceleration pulses.

DISCUSSION

Finite element modeling is a formidable asset for the study of traumatic brain injuries, as it allows obtaining numerical data about the mechanical response of the brain, which would otherwise be experimentally almost impossible. For example, region-specific intrinsic parameters such as stresses and strains cannot be experimentally measured. These metrics are important in differentiating the response of different components to the external insult. Based on regional biomechanical variables it is possible to support clinically-postulated injury mechanisms and derive tolerance criteria. A similar approach has been used in finite element modeling of the pediatric and adult spine to understand the intrinsic responses (Kumaresan et al., 1999; Kumaresan et al., 2001; Kumaresan et al., 1997; Yoganandan et al., 1996). Existing methodologies for directly measuring some of these variables, particularly in the rat, are challenging and can confound the total mechanical response of the brain and affect injury/behavioral outcomes.

As a consequence, it has been used in various applications. With regard to finite element modeling of the rat brain, Dynamic Cortical Deformations (DCD) (Shreiber et al., 1997) were used to study injuries to the blood-brain barrier, Controlled Cortical Impacts (CCI) (Gefen et al., 2003; Levchakov et al., 2006) were used to determine stress and strain distributions and complement experimental indentation data, and a high definition model (Mao et al., 2006) was used to study DCD and CCI. In addition, a two-dimensional FEM was used to model experimental protocols described here (Fijalkowski et al., 2009b). However, to our knowledge, the present model is the first complete three dimensional model incorporated in the study of mild TBI sustained during pure angular acceleration loading with stress response verified using behavioral and pathological outcomes.

Von Mises stresses proved to be an indicator of injury, as distribution in the FEM matched observed outcomes of the experimental setup, with a particular emphasis on the hippocampus. Correlation between Von Mises stress and observed neurological injuries was previously identified in sheep (Anderson et al., 2003; Anderson et al., 1999) and other animals as well as for human (Baumgartner and Willinger, 2004; Marjoux et al., 2008).

Peak Von Mises stresses demonstrated consistency with regard to the magnitude of angular acceleration. With stresses considered as indicators of the level of injury, this result could signify that the present model could serve to determine injury thresholds based on Von Mises stresses. Correlations with experimental histological observations and behaviors add to the validity of this metric for injury determination. Recent studies have shown that the brain response is both region- and pulse shape-dependent. Exercising a two-dimensional model under pure rotational accelerations, it has been shown that the stress-strain

response depends both on the amplitude and duration of the applied pulse (Fijalkowski et al., 2009b; Yoganandan et al., 2008). While peak Von Mises stresses concurred with increasing abnormalities associated with increasing acceleration magnitudes, this metric did not follow a similar tendency with the duration abscissa. Shorter times induced greater jerks in the input for a given acceleration, perhaps increasing the instantaneous stress magnitudes.

This is the reason why the stress-time variable was introduced. Indeed, knowing the value of the applied stress is a first insight into the possible consequences suffered by the brain. But, should this value be obtained for an instantaneous peak, or maintained for a given duration, the severity will obviously be quite different. The inclusion of a time-based indication, by integrating the Von Mises stress to obtain the stress-time, provides a metric which is closer to a global influence of the mechanical insult on the brain, to the total energy it receives. A point of comparison can be made with criterions such as the Head Injury Criterion, which evaluates the risks sustained by the head in a collision case by implicitly taking into account the amplitude of the acceleration and its duration (NHTSA, 2003). As time and acceleration implicitly involve rotational velocity, a criterion with two of these variables includes the effect of the other parameter. Although not quantitatively proposed, a rotation-based metric similar to HIC may be derived by incorporating velocity instead of, or in addition to, peak acceleration.

Apart from the peak magnitudes of the mechanical responses, the other significant result was the anatomical location. Peak stresses and stress-times were greatest in the hippocampus, the anatomical region demonstrating the most remarkable histological findings in the current experimental series. It is well known for humans and rats that the hippocampus is responsible for cognitive and spatial navigation functions. It has been demonstrated, through patho-physiological findings, to be one of the most affected brain regions in TBI cases (Otani et al., 2011). The Morris water maze (Morris et al., 1982) is a commonly used test to assess spatial learning deficits associated with hippocampal injury. Rats sustaining TBI have demonstrated performance deficits compared to uninjured rats (Hamm et al., 1992; Morris et al., 1982). These types of deficits are a common clinical outcome in patients with mild TBI (NHTSA, 2003).

Injury to other brain regions do not manifest as these types of neurological changes (Hamm et al., 1993), underlining the particular sensitivity of the hippocampus to mechanical stresses sustained during mild TBI-induced angular acceleration levels. Memory deficits have been associated with multiple indicators of hippocampal damage including neuro-pathological changes (Hicks et al., 1996; Hicks et al., 1993) through neuronal cell death (Raghupathi et al., 2000; Smith et al., 1991; Smith et al., 1995). The present analysis demonstrated that the stress-time metric may be responsible for local mechanical changes in the hippocampus leading to these biological variations. Therefore, as has been shown for greater injury severities (AIS 4-6), biomechanical metrics may also be responsible for modulating injury severity and the ensuing patho-biological processes following mild TBI (AIS 2-3).

Comparison of experimental and numerical results has demonstrated afore discussed correlations between stress response and pathological outcomes. Nevertheless, finite element modeling has limitations. First of all are the chosen material simplifications. As a first step, the present model incorporated isotropic and homogeneous material properties, because experimental data do not exist for each anatomical region of the rat brain. It is known for other species that gray and white matter material properties differ. The interior components of the FEM were created such that it is possible to implement different properties for the two components. It should be stressed that white matter properties remain scarce and varied: depending on models, white matter can be considered softer than gray matter (Mao et al., 2006; Prange and Margulies, 2002), as well as stiffer (Fijalkowski et al., 2009b). Since the increase or decrease in stiffness is generally assumed to be 20% of gray matter, it was decided to maintain the homogeneity assumption. Another aspect of the model is the material law. Although linear viscous elasticity is the most commonly used material law for FEM of the rat brain, improvements could be obtained by incorporating nonlinear viscous elastic behavior (Brands and Bovendeerd, 2002). Besides, diffusion tensor imaging can be used to quantify anisotropic properties (Colgan et al., 2010). These modifications could be undertaken in future enhancements of the present three dimensional finite element model of the rat brain.

Finite element modeling also permits variation of the solicitation. Angular accelerations have been accepted as a major cause of brain injury (Gennarelli et al., 1982). Nevertheless, no real collision would generate only angular accelerations without a linear component (Yoganandan et al., 2009). A future use

of the present FEM would be to recreate linear acceleration cases. Simulations involving both linear and angular components could also be considered, but they would be hampered by the impossibility to discern one from the other in terms of causality of the observed outcomes (Li et al., 2010). However, in terms of delineating injury thresholds, the present simplified focus on only one component remains a viable alternative to studying realistic and complex mechanics of mild TBI.

Despite these limitations, the experimental and finite element models offer a good correlation. The long term goal will be to extrapolate results from rat to human models, to glean further knowledge on mechanisms of mild TBI which may be used for improving safety in automotive environments. As of now, present results underscore the role of the pulse shape from an external perspective such as airbag versus A-pillar loading in frontal impacts, bonnet-to-head versus windshield-to-head impacts in pedestrians associated with differing external vehicle geometries, helmet-to-road contact versus head-to-road contact in motorcycle crashes, and a similar role in the intrinsic brain response (e.g., peak stresses versus an integrated measure of stress-time). An implication would be to develop a new criterion incorporating time into the intracranial response, which could improve brain injury assessments in automotive environments.

CONCLUSION

A three dimensional finite element model of the rat skull and brain was used to understand the anatomical region-dependent stress response of the brain under mild TBI conditions. Stress response metrics were correlated to histological and behavioral (e.g., loss of consciousness) evidence of injury in rats subjected to pure coronal plane angular acceleration of the head. Injury severity was modulated by independently controlling peak magnitude and duration of the angular acceleration. While peak Von Mises stresses correlated well with changes in injury severity associated with peak angular acceleration, this metric did not demonstrate sensitivity to changes in angular acceleration duration. However, an integrated stress-time metric was able to predict changes in injury severity associated with increasing angular acceleration magnitude as well as duration in both the hippocampal and parietal cortex anatomical regions. Results of this unique hybrid analysis indicate that the combined stress-time variable may be more suited to explain variation of mild TBI severity, rather than pure peak metrics.

ACKNOWLEDGMENTS

This research was supported in part by the Veterans Affairs Medical Research and the Department of Neurosurgery, Medical College of Wisconsin.

REFERENCES

Anderson RW, Brown CJ, Blumbergs PC, McLean AJ, Jones NR. 2003. Impact mechanics and axonal injury in a sheep model. J Neurotrauma 20:961-974.

Anderson RW, Brown CJ, Blumbergs PC, Scott G, Finnie J, Jones NR, McLean AJ. 1999. Mechanisms of axonal injury: an experimental and numerical study of a sheep model of head impact. In: Proceedings of the IRCOBI Conference. p 107-120.

Baumgartner D, Lamy M, Willinger R, Choquet T, Goetz C, Constantinesco A. 2009. Finite element analysis of traumatic brain injuries mechanisms in the rat. In: Proceedings of the IRCOBI Conference. p 97-108.

Baumgartner D, Willinger R. 2004. Human head tolerance limits to specific injury mechanisms inferred from real world accident numerical reconstruction. Revue Europeenne des Elements Finis 14:421-444.

Brands DW, Bovendeerd P. 2002. On the potential importance of non-linear viscoelastic material modelling for numerical prediction of brain tissue response: test and application.

Cassidy JD, Carroll LJ, Peloso PM, Borg J, von Holst H, Holm L, Kraus J, Coronado VG. 2004. Incidence, risk factors and prevention of mild traumatic brain injury: results of the WHO Collaborating Centre Task Force on Mild Traumatic Brain Injury. J Rehabil Med:28-60.

Colgan NC, Gilchrist MD, Curran KM. 2010. Applying DTI white matter orientations to finite element head models to examine diffuse TBI under high rotational accelerations. Prog Biophys Mol Biol 103:304-309.

Fijalkowski RJ, Ellingson BM, Stemper BD, Yoganandan N, Gennarelli TA, Pintar FA. 2006. Interface parameters of impact-induced mild traumatic brain injury. Biomed Sci Instrum 42:108-113.

Fijalkowski RJ, Ropella KM, Stemper BD. 2009a. Determination of low-pass filter cutoff frequencies for high-rate biomechanical

signals obtained using videographic analysis. J Biomech Eng 131:054502.

Fijalkowski RJ, Stemper BD, Pintar FA, Yoganandan N, Crowe MJ, Gennarelli TA. 2007. New rat model for diffuse brain injury using coronal plane angular acceleration. J Neurotrauma 24:1387-1398.

Fijalkowski RJ, Yoganandan N, Zhang J, Pintar FA. 2009b. A finite element model of region-specific response for mild diffuse brain injury. Stapp Car Crash J 53:193-213.

Gefen A, Gefen N, Zhu Q, Raghupathi R, Margulies SS. 2003. Age-dependent changes in material properties of the brain and braincase of the rat. J Neurotrauma 20:1163-1177.

Gennarelli TA, Adams JH, Graham DI. 1981. Acceleration induced head injury in the monkey.I. The model, its mechanical and physiological correlates. Acta Neuropathol Suppl 7:23-25.

Gennarelli TA, Thibault LE, Adams JH, Graham DI, Thompson CJ, Marcincin RP. 1982. Diffuse axonal injury and traumatic coma in the primate. Annals of Neurology 12:564-574.

Gennarelli TA, Wodzin E. 2006. AIS 2005: a contemporary injury scale. Injury 37:1083-1091.

Hahn N, Eisen RJ, Eisen L, Lane RS. 2005. Ketamine-medetomidine anesthesia with atipamezole reversal: practical anesthesia for rodents under field conditions. Lab Anim (NY) 34:48-51.

Hamm RJ, Dixon CE, Gbadebo DM, Singha AK, Jenkins LW, Lyeth BG, Hayes RL. 1992. Cognitive deficits following traumatic brain injury produced by controlled cortical impact. J Neurotrauma 9:11-20.

Hamm RJ, Lyeth BG, Jenkins LW, O'Dell DM, Pike BR. 1993. Selective cognitive impairment following traumatic brain injury in rats. Behav Brain Res 59:169-173.

Hicks R, Soares H, Smith D, McIntosh T. 1996. Temporal and spatial characterization of neuronal injury following lateral fluid-percussion brain injury in the rat. Acta Neuropathol 91:236-246.

Hicks RR, Smith DH, Lowenstein DH, Saint Marie R, McIntosh TK. 1993. Mild experimental brain injury in the rat induces cognitive deficits associated with regional neuronal loss in the hippocampus. J Neurotrauma 10:405-414.

Holbourn AHS. 1943. Mechanics of Head Injuries. The Lancet 242:438-441.

Kumaresan S, Yoganandan N, Pintar FA, Maiman DJ. 1999. Finite element modeling of the cervical spine: role of intervertebral disc under axial and eccentric loads. Med Eng Phys 21:689-700.

Kumaresan S, Yoganandan N, Pintar FA, Maiman DJ, Goel VK. 2001. Contribution of disc degeneration to osteophyte formation in the cervical spine: a biomechanical investigation. J Orthop Res 19:977-984.

Kumaresan S, Yoganandan N, Pintar FA, Voo LM, Cusick JF, Larson SJ. 1997. Finite element modeling of cervical laminectomy with graded facetectomy. J Spinal Disord 10:40-46.

Levchakov A, Linder-Ganz E, Raghupathi R, Margulies SS, Gefen A. 2006. Computational studies of strain exposures in neonate and mature rat brains during closed head impact. J. Neurotrauma 23:1570-1580.

Li XY, Li J, Feng DF, Gu L. 2010. Diffuse axonal injury induced by simultaneous moderate linear and angular head accelerations in rats. Neuroscience 169:357-369.

Lissner HR, Lebow M, Evans FG. 1960. Experimental studies on the relation between acceleration and intracranial pressure changes in man. Surg Gynecol Obstet 111:329-338.

Mao H, Zhang L, Yang KH, King AI. 2006. Application of a finite element model of the brain to study traumatic brain injury mechanisms in the rat. Stapp Car Crash J 50:583-600.

Marjoux D, Baumgartner D, Deck C, Willinger R. 2008. Head injury prediction capability of the HIC, HIP, SIMon and ULP criteria. Accid Anal Prev 40:1135-1148.

Morris RG, Garrud P, Rawlins JN, O'Keefe J. 1982. Place navigation impaired in rats with hippocampal lesions. Nature 297:681-683.

NHTSA. 2003. www.nhtsa.dot.gov. In. Washington, DC, USA: The United States Department of Transportation.

Otani N, Nawashiro H, Shima K. 2011. Pathophysiological findings of selective vulnerability in the hippocampus after traumatic brain injury. J Exp Clin Med 3:22-26.

Prange MT, Margulies SS. 2002. Regional, directional, and age-dependent properties of

the brain undergoing large deformation. J Biomech Eng 124:244-252.

Radioss. 2009. Theory manual 10.0 version. Altair Engineering, Inc. In.

Raghupathi R, Graham DI, McIntosh TK. 2000. Apoptosis after traumatic brain injury. J Neurotrauma 17:927-938.

Shreiber DI, Bain AC, Meaney DF. 1997. In vivo thresholds for mechanical injury to the blood-brain barrier. In: 41st Stapp Car Crash Conf. p 277-292.

Smith DH, Okiyama K, Thomas MJ, Claussen B, McIntosh TK. 1991. Evaluation of memory dysfunction following experimental brain injury using the Morris water maze. J Neurotrauma 8:259-269.

Smith DH, Soares HD, Pierce JS, Perlman KG, Saatman KE, Meaney DF, Dixon CE, McIntosh TK. 1995. A model of parasagittal controlled cortical impact in the mouse: cognitive and histopathologic effects. J Neurotrauma 12:169-178.

Sun FJ, Wright DE, Pinson DM. 2003. Comparison of ketamine versus combination of ketamine and medetomidine in injectable anesthetic protocols: chemical immobilization in macaques and tissue reaction in rats. Contemp Top Lab Anim Sci 42:32-37.

Tagliaferri F, Compagnone C, Korsic M, Servadei F, Kraus J. 2006. A systematic review of brain injury epidemiology in Europe. Acta Neurochir (Wien) 148:255-268; discussion 268.

Yoganandan N, Gennarelli TA, Zhang J, Pintar FA, Takhounts E, Ridella SA. 2009. Association of contact loading in diffuse axonal injuries from motor vehicle crashes. J Trauma 66:309-315.

Yoganandan N, Kumaresan S, Voo L, Pintar FA. 1996. Finite element applications in human cervical spine modeling. Spine (Phila Pa 1976) 21:1824-1834.

Yoganandan N, Li J, Zhang J, Pintar FA, Gennarelli TA. 2008. Influence of angular acceleration-deceleration pulse shapes on regional brain strains. J Biomech 41:2253-2262.

Zhang J, Yoganandan N, Pintar FA, Gennarelli TA. 2006. Brain strains in vehicle impact tests. Annu Proc Assoc Adv Automot Med 50:1-12.